RESEARCH ARTICLE

QUANTUM OPTICS

Satellite-based entanglement distribution over 1200 kilometers

Juan Yin,[1,2] Yuan Cao,[1,2] Yu-Huai Li,[1,2] Sheng-Kai Liao,[1,2] Liang Zhang,[2,3] Ji-Gang Ren,[1,2] Wen-Qi Cai,[1,2] Wei-Yue Liu,[1,2] Bo Li,[1,2] Hui Dai,[1,2] Guang-Bing Li,[1,2] Qi-Ming Lu,[1,2] Yun-Hong Gong,[1,2] Yu Xu,[1,2] Shuang-Lin Li,[1,2] Feng-Zhi Li,[1,2] Ya-Yun Yin,[1,2] Zi-Qing Jiang,[3] Ming Li,[3] Jian-Jun Jia,[3] Ge Ren,[4] Dong He,[4] Yi-Lin Zhou,[5] Xiao-Xiang Zhang,[6] Na Wang,[7] Xiang Chang,[8] Zhen-Cai Zhu,[5] Nai-Le Liu,[1,2] Yu-Ao Chen,[1,2] Chao-Yang Lu,[1,2] Rong Shu,[2,3] Cheng-Zhi Peng,[1,2]* Jian-Yu Wang,[2,3]* Jian-Wei Pan[1,2]*

Long-distance entanglement distribution is essential for both foundational tests of quantum physics and scalable quantum networks. Owing to channel loss, however, the previously achieved distance was limited to ~100 kilometers. Here we demonstrate satellite-based distribution of entangled photon pairs to two locations separated by 1203 kilometers on Earth, through two satellite-to-ground downlinks with a summed length varying from 1600 to 2400 kilometers. We observed a survival of two-photon entanglement and a violation of Bell inequality by 2.37 ± 0.09 under strict Einstein locality conditions. The obtained effective link efficiency is orders of magnitude higher than that of the direct bidirectional transmission of the two photons through telecommunication fibers.

Quantum entanglement, first recognized by Einstein, Podolsky, and Roson (*1*) and Schrödinger (*2*), is a physical phenomenon in which the quantum states of a many-particle system cannot be factorized into a product of single-particle wave functions, even when the particles are separated by large distances. Entangled states have been produced in laboratories (*3*–*5*) and exploited to test the contradiction between classical local hidden variable theory and quantum mechanics by using Bell's inequality (*6*). It is of fundamental interest to distribute entangled particles over increasingly large distances and study the behavior of entanglement under extreme conditions. Practically, large-scale dissemination of entanglement—eventually at a global scale—is useful as the essential physical resource for quantum information protocols such as quantum cryptography (*7*), quantum teleportation (*8*), and quantum networks (*9*).

Limitations on entanglement distribution

So far, entanglement distribution has only been achieved at a physical separation up to ~100 km (*10*) and is mainly limited by the photon loss in the channel (optical fibers or terrestrial free space), which normally scales exponentially with the channel length. For example, through bidirectional distribution of an entangled source of photon pairs with a 10-MHz count rate directly through two 600-km telecommunication fibers with a loss of 0.16 dB/km, eventually one would only obtain 10^{-12} two-photon coincidence events per second. When the transmitted photons are attenuated to a level comparable to the dark counts of the single-photon detectors, the entanglement cannot be established because of the low signal-to-noise ratio. To improve the signal-to-noise ratio, the entangled photons in the channel cannot simply be amplified because of the quantum noncloning theorem (*11*), but radically new methods to reduce the link attenuation must be developed.

One solution to improve the distribution is the protocol of quantum repeaters (*12*) that divide the whole transmission line into smaller segments and combine the functionalities of entanglement swapping (*13*), entanglement purification (*14*), and quantum storage (*15*). There has been considerable progress in the demonstrations of these building blocks (*16*–*18*) and proof-of-principle quantum repeater nodes (*19*, *20*). However, the practical usefulness of the quantum repeaters is still hindered by the challenges of simultaneously realizing and integrating all the key capabilities, including, most importantly, long storage time and high retrieval efficiency (*21*).

Satellite-based entanglement distribution

Another approach to global-scale quantum networks is making use of satellite- and space-based technologies. A satellite can conveniently cover two distant locations on Earth separated by thousands of kilometers. The key advantage of this approach is that the photon loss and turbulence predominantly occur in the lower ~10 km of the

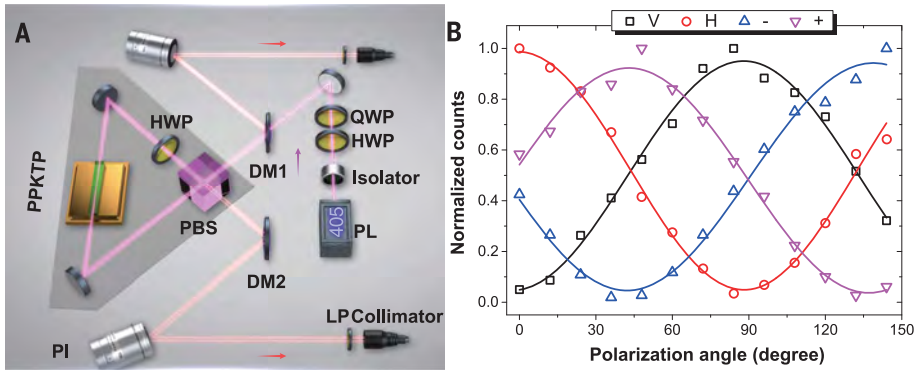

Fig. 1. Schematic of the spaceborne entangled-photon source and its in-orbit performance. (**A**) The thickness of the $KTiOPO_4$ (PPKTP) crystal is 15 mm. A pair of off-axis concave mirrors focus the pump laser (PL) in the center of the PPKTP crystal. At the output of the Sagnac interferometer, two dichromatic mirrors (DMs) and long-pass filters are used to separate the signal photons from the pump laser. Two additional electrically driven piezo steering mirrors (PIs), remotely controllable on the ground, are used for fine adjustment of the beam-pointing for an optimal collection efficiency into the single-mode fibers. QWP, quarter-wave plate; HWP, half-wave plate; PBS, polarizing beam splitter. (**B**) The two-photon correlation curves measured on-satellite by sampling 1% of each path of the entangled photons. The count rate measured from the overall 0.01% sampling is about 590 Hz, from which we can estimate the source brightness of 5.9 MHz.

[1]Department of Modern Physics and Hefei National Laboratory for Physical Sciences at the Microscale, University of Science and Technology of China, Hefei 230026, China. [2]Chinese Academy of Sciences (CAS) Center for Excellence and Synergetic Innovation Center in Quantum Information and Quantum Physics, University of Science and Technology of China, Shanghai 201315, China. [3]Key Laboratory of Space Active Opto-Electronic Technology, Shanghai Institute of Technical Physics, Chinese Academy of Sciences, Shanghai 200083, China. [4]Key Laboratory of Optical Engineering, Institute of Optics and Electronics, Chinese Academy of Sciences, Chengdu 610209, China. [5]Shanghai Engineering Center for Microsatellites, Shanghai 201203, China. [6]Key Laboratory of Space Object and Debris Observation, Purple Mountain Observatory, Chinese Academy of Sciences, Nanjing 210008, China. [7]Xinjiang Astronomical Observatory, Chinese Academy of Sciences, Urumqi 830011, China. [8]Yunnan Observatories, Chinese Academy of Sciences, Kunming 650011, China.
***Corresponding author. Email: pcz@ustc.edu.cn (C.-Z.P.); jywang@mail.sitp.ac.cn (J.-Y.W.); pan@ustc.edu.cn (J.-W.P.)**

atmosphere, and most of the photons' transmission path is virtually in vacuum, with almost zero absorption and decoherence. Previously, ground-based feasibility studies have demonstrated bidirectional distribution of entangled photon pairs through a two-link terrestrial free-space channel—with violations of Bell inequality—over distances of 600 m (*22*); 13 km, which goes beyond the effective atmospheric thickness (*23*); and 102 km with an ~80-dB effective channel loss, comparable to that of a satellite-to-ground two-downlink channel (*10*). In addition, quantum communications on moving platforms in a high-loss regime and under turbulent conditions were also tested (*24*, *25*). After these feasibility studies, a satellite dedicated for quantum science experiments, Micius [see the supplementary materials (*26*)], was developed and launched from Jiuquan, China, to an altitude of ~500 km.

For the mission of entanglement distribution, three ground stations are cooperating with the satellite, located in Delingha in Qinghai (37°22′44.43″N, 97°43′37.01″E; altitude, 3153 m); Nanshan in Urumqi, Xinjiang (43°28′31.66″N, 87°10′36.07″E; altitude, 2028 m); and Gaomeigu Observatory in Lijiang, Yunnan (26°41′38.15″N, 100°1′45.55″E; altitude, 3233 m). The physical distance between Delingha and Lijiang (Nanshan) is 1203 km (1120 km). The separation between the orbiting satellite and these ground stations varies from 500 to 2000 km. The effective laboratory space is thus greatly increased and provides a new platform for quantum networks, as well as for probing the validity of quantum mechanics.

By developing an ultrabright spaceborne two-photon entanglement source and high-precision acquiring, pointing, and tracking (APT) technology, we established entanglement between two single photons separated by 1203 km, with an average two-photon count rate of 1.1 Hz and state fidelity of 0.869 ± 0.085. Using the distributed entangled photons, we performed the Bell test at spacelike separation and without the locality and the freedom-of-choice loopholes.

Spaceborne entangled photons

In our design of a spaceborne entangled-photon source (Fig. 1A), a continuous-wave laser diode with a central wavelength of 405 nm and a linewidth of ~160 MHz is used to pump a periodically poled $KTiOPO_4$ crystal inside a Sagnac interferometer. The pump laser, split by a polarizing beam splitter, passes through the nonlinear crystal in the clockwise and anticlockwise directions simultaneously, which produces down-converted photon pairs at a wavelength of ~810 nm in polarization-entangled states close to the form $|\psi\rangle_{1,2} = (|H\rangle_1|V\rangle_2 + |V\rangle_1|H\rangle_2)/\sqrt{2}$, where $|H\rangle$ and $|V\rangle$ denote the horizontal and vertical polarization states, respectively, and the subscripts 1 and 2 denote the two output spatial modes. This source is robust against various vibration, temperature, and electromagnetic conditions (*26*). After launch, the source brightness and fidelity were tested by sampling ~1% of each path of the entangled photon pairs for on-satellite analysis (Fig. 1B). Under a pump power of ~30 mW, the source emits 5.9 million entangled photon pairs per second, with a state fidelity of 0.907 ± 0.007.

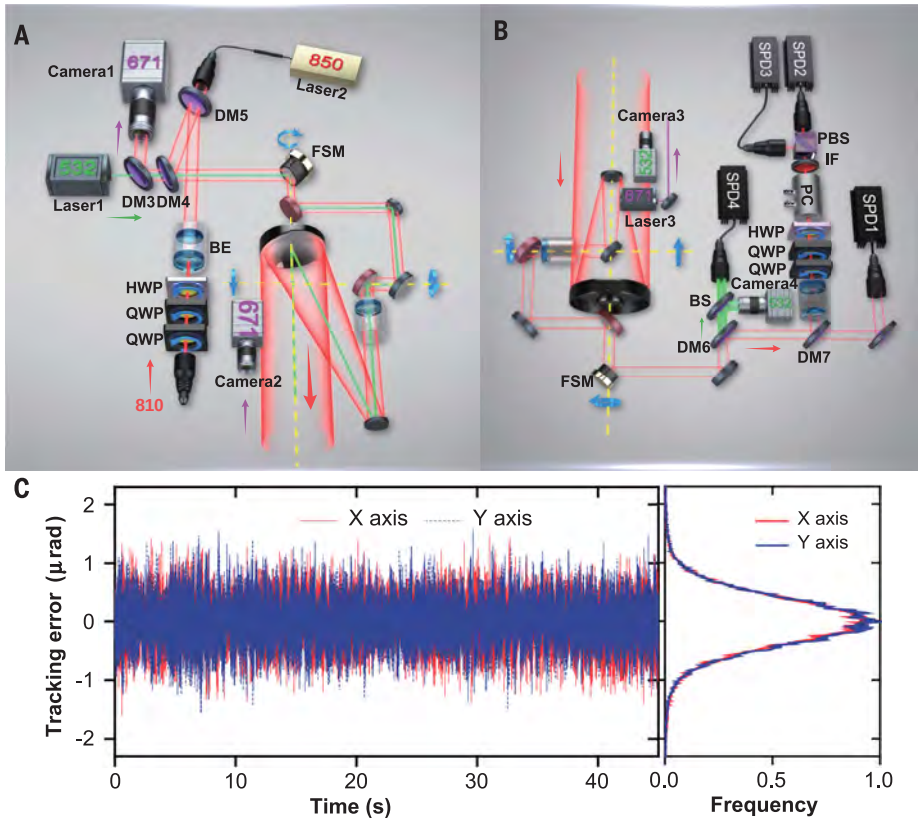

Fig. 2. The transmitters, receivers, and APT performance. (**A**) The entangled-photon beam (810 nm) is combined and co-aligned with a pulsed infrared laser (850 nm) for synchronization and a green laser (532 nm) for tracking by three DMs and sent out from an 8× telescope. For polarization compensation, two motorized QWPs and a HWP are remotely controlled. A fast steering mirror (FSM) and a two-axis turntable are used for closed-loop fine and coarse tracking, based on the 671-nm beacon laser images captured by cameras 1 and 2. BE, beam expander. (**B**) Schematic of the receiver at Delingha. The cooperating APT and polarization compensation systems are the same as those on the satellite. The tracking and synchronization lasers are separate from the signal photon and detected by single-photon detectors (SPDs). For polarization analysis along bases that are randomly switching quickly, two QWPs, a HWP, a Pockels cell (PC), and a PBS are used. BS, beam splitter; IF, interference filter. (**C**) The APT system starts tracking after the satellite reaches a 5° elevation angle. The left panel is a 50-s trace of the real-time image readout from the camera. Fine-tracking accuracy of ~0.41 μrad is achieved for both the *x* and *y* axes.

Establishing a space-to-ground two-downlink channel

As the entangled photons propagate from the satellite through the atmosphere to the two ground stations, each with a travel distance of 500 to 2000 km, several effects contribute to channel loss, including beam diffraction, pointing error, atmospheric turbulence, and absorption. Because the entangled photons cannot be amplified as classical signals, a robust and efficient satellite-to-ground entanglement distribution places more stringent requirements on the link efficiency than conventional satellite-based classical communications do. In particular, a satellite payload with two telescopes capable of establishing two independent satellite-to-ground quantum links simultaneously is required.

To optimize the link efficiency, we combined a narrow beam divergence with a high-bandwidth and high-precision APT technique. The two entangled beams were sent out with a near-diffraction-limited far-field divergence of ~10 μrad by two Cassegrain telescopes with apertures of 300 and 180 mm (Fig. 2A), which have been optimized to eliminate chromatic and spherical abbreviations at a wavelength of ~810 nm. The overall optical efficiencies of the two telescopes are 45 to 55%. At the Delingha, Lijiang, and Nanshan stations, the receiving telescopes have diameters of 1200, 1800, and 1200 mm, respectively. Our experiment has achieved entanglement distribution both between Delingha and Lijiang and between Delingha and Nanshan (*26*).

We designed cascaded multistage closed-loop APT systems in both the transmitters (Fig. 2A) and receivers (Fig. 2B). The transmitters use green (~532 nm) beacon lasers, whereas the receivers

use red (~671 nm) beacon lasers, pointing to each other with a divergence of ~1.2 mrad. The coarse pointing stages consist of a two-axis turntable or gimbal mirror and wide field-of-view cameras, and they achieve an accuracy better than 50 μrad. Further, the fine pointing stages with fast-steering mirrors and high-speed cameras reliably lock the remote telescopes by a feedback closed loop with a measured accuracy of 0.41 μrad for both the x and y axes (Fig. 2C), much smaller than the beam divergence (*26*). The APT systems are started when the satellite reaches a 5° elevation angle, and the measurement begins when it reaches a 10° elevation angle.

The motion of the satellite relative to the ground induces a drift in the arrival time and polarization rotation observed by the receivers. We kept track of the relative motion between the transmitters and the receivers, as well as all the optical elements in the optical paths, to calculate the polarization rotation angle offset and phase shift. Using a combination of motorized wave plates (two quarter-wave plates and one half-wave plate) for dynamical polarization compensation (*26*), we were able to recover the polarization contrast to 80:1. Synchronization of two ground stations was done with a 100-kHz pulsed laser, sent from the satellite and in good co-alignment with the signal photons. A synchronization jitter of 0.77 ns was obtained, which was used to tag the received signals and perform coincidence detection within a 2.5-ns time window. In addition to the temporal filtering, we placed 20-nm bandwidth filters in the receiving telescope to reduce the background noise. In our experiment, depending on the position of the Moon, the background noise ranged from 500 to 2000 counts/s in each detector.

The satellite flies along a sun-synchronous orbit and comes into both Delingha's and Lijiang's views once every night, starting at around 1:30 AM Beijing time and lasting for a duration of ~275 s. Figure 3A plots the physical distances from the satellite to Delingha and Lijiang during one orbit, together with the summed channel length of the two downlinks. Using a reference laser (*26*) on the satellite, we measured in real time the overall two-downlink channel attenuation, which varies from 64 to 82 dB (Fig. 3B). A slight asymmetry is evident in the attenuation curve—when the satellite moves closer to Lijiang, the link efficiency is higher, which is because the Lijiang station has a larger-aperture telescope. We observed an average two-photon count rate of 1.1 Hz, with a signal-to-noise ratio of ~8:1.

Compared with the previous method of entanglement distribution by direct transmission of the same two-photon source—using the best-performance (with a loss of 0.16 dB/km) and most common (with a loss of 0.2 dB/km) commercial telecommunication fibers, respectively—the effective link efficiency of our satellite-based approach within the 275-s coverage time is 12 and 17 orders of magnitude higher (*27*). The intrinsic physical loss limit of the silica optical fibers is estimated to be 0.095 to 0.13 dB/km (*28*). Even if such perfect optical fibers were produced in the future, our satellite-based method would still be four to eight orders of magnitude more efficient. In the future, satellites at higher orbits are expected to increase the area and time coverage.

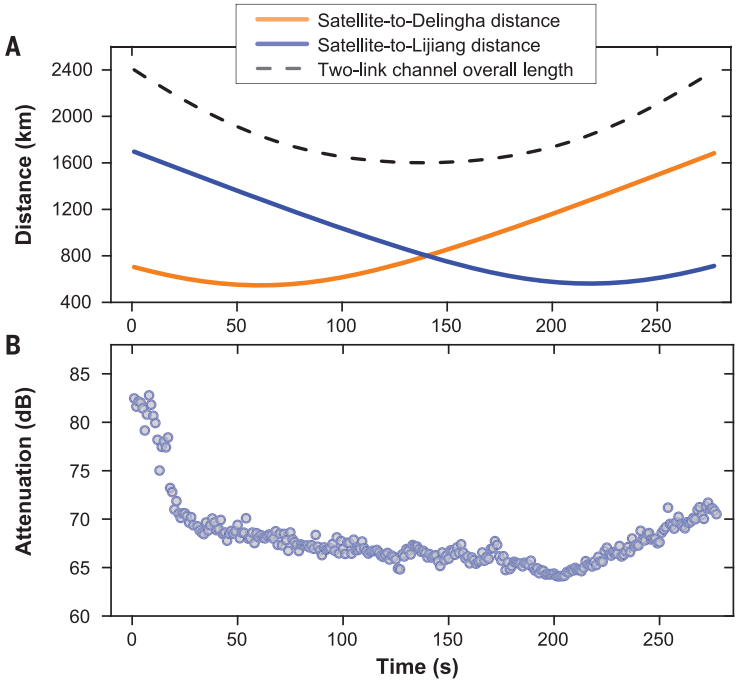

Fig. 3. Physical distances from the satellite to two ground stations and the measured channel attenuation. (**A**) A typical two-downlink transmission from the satellite to Delingha and Lijiang that lasted for about 275 s in one orbit. The distance from the satellite to Delingha varies from 545 to 1680 km. The distance from the satellite to Lijiang varies from 560 to 1700 km. The overall length of the two-downlink channel varies from 1600 to 2400 km. (**B**) The measured two-downlink channel attenuation in one orbit, using the high-intensity reference laser co-aligned with the entangled photons. The highest loss is ~82 dB at the summed distance of 2400 km, when the satellite has just reached a 10° elevation angle as seen from Lijiang station. Because the telescope has a diameter of 1.8 m (the largest) and thus has a higher receiving efficiency than other stations, when the satellite flies over Lijiang at an elevation angle of more than 15°, the channel loss remains relatively stable, from 64 to 68.5 dB.

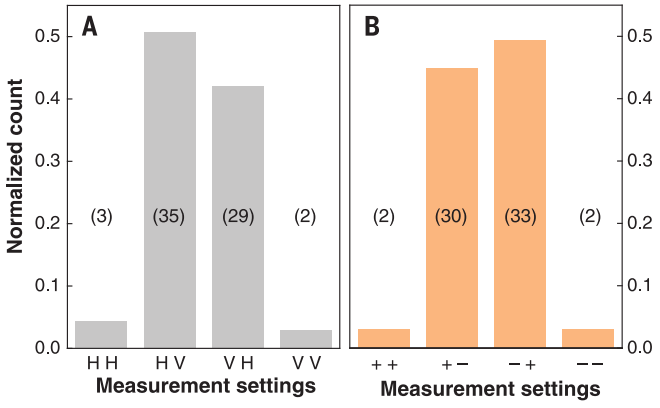

Fig. 4. Measurement of the received entangled photons after transmission by the two-downlink channel. (**A**) Normalized two-photon coincidence counts in the measurement setting of the $|H\rangle/|V\rangle$ basis. (**B**) Normalized counts in the diagonal $|\pm\rangle$ basis. Numbers in parentheses represent the raw coincidence counts of different measurement settings.

Verifying entanglement and Bell test

The received photons were analyzed by a half-wave plate, a polarizing beam splitter, and a Pockels cell, then coupled into a multimode fiber and detected by single-photon detectors with low dark counts (<100 Hz). The Pockels cells were driven by high-voltage pulses rapidly switching between zero- and half-wave voltages, controlled by fast (4 megabits/s) random numbers. Such a setting allows measurements of polarization at the basis of $\cos\theta|H\rangle + \sin\theta|V\rangle$. To verify whether the two photons, after traveling the overall distance ranging from 1600 to 2400 km, were still entangled, we analyzed their polarizations in the $|H\rangle/|V\rangle$

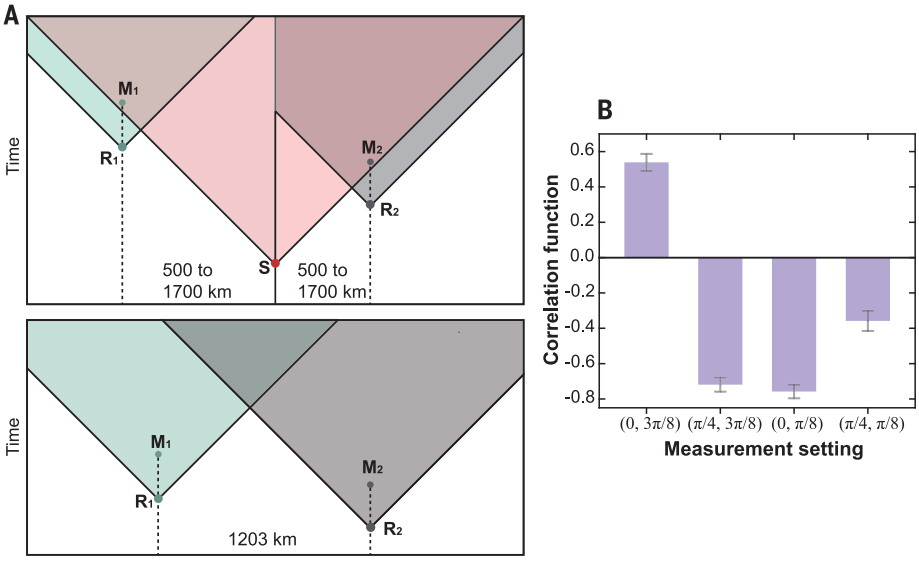

Fig. 5. Space-time diagram and Bell inequality violation. (**A**) The top panel illustrates the space-time relationship among the entanglement generation point (S), the quantum random-number generation points (R1 and R2), and the measurement results points (M1 and M2). The horizontal axis represents the distances between the ground stations and the satellite, which vary from 500 to 1700 km. In our experimental configuration, M1 and M2 are about 100 ns behind the light cone of S. The rate of quantum random-number generation is 5 kHz with an output delay below 200 ns. That is, the duration between R1 (R2) and M1 (M2) is in the range of 0.2 to 200.2 μs. Therefore, R1 (R2) and S are spacelike-separated, which implies that the freedom-of-choice loophole is distinctly closed, under the additional assumption that all the possible hidden variables must originate together with the entangled particles. The bottom panel illustrates the relationship between two ground stations, which are 1203 km apart. Taking into account the orbit height of 500 km, the length difference between the two free-space channels does not exceed 944 km. Thus, the spacelike criterion is satisfied between R1 and R2, R1 and M2, M1 and R2, and M1 and M2. As a result, the locality loophole is addressed. (**B**) Correlation functions of a CHSH-type Bell inequality for entanglement distribution. The measurement settings are the angles (φ_1, φ_2) used for the measurement of the polarization of photons by the Delingha and Lijiang stations, respectively. Error bars are one standard deviation, calculated from propagated Poissonian counting statistics of the raw photon detection events.

and $|\pm\rangle = (|H\rangle \pm |V\rangle)/\sqrt{2}$ bases. We obtained 134 coincidence counts—raw data without subtracting background noise—during an effective time of 250 s in satellite-orbit shadow time (Fig. 4). We found that, in good agreement with the state $|\psi\rangle_{1,2}$, the $|H\rangle_1|V\rangle_2$ and $|V\rangle_1|H\rangle_2$ populations dominate in the $|H\rangle/|V\rangle$ basis (Fig. 4A). Further, the coherence of the state is evident in Fig. 4B, where the measured $|+\rangle_1|+\rangle_2$ and $|-\rangle_1|-\rangle_2$ counts dominate over $|+\rangle_1|-\rangle_2$ and $|-\rangle_1|+\rangle_2$ at a ratio of 16:1. From these measurements, we can estimate the state fidelity [defined as the wave function overlap of the experimentally obtained states with the ideal $|\psi\rangle_{1,2}$ (*29*)] of the two photons distributed over 1203 km: $F \geq 0.87 \pm 0.09$, which is well above the threshold for both confirming the two-particle entanglement and violating Bell inequalities.

We used the distributed entangled photons for the Bell test with the Clauser-Horne-Shimony-Holt (CHSH)–type inequality (*30*), which is given by

$$S = |E(\varphi_1,\varphi_2) - E(\varphi_1,\varphi_2') + E(\varphi_1',\varphi_2) + E(\varphi_1',\varphi_2')| \leq 2$$

where $E(\varphi_1,\varphi_2)$, $E(\varphi_1,\varphi_2')$, and so forth are the joint correlations at the two remote locations with respective measurement angles of (φ_1,φ_2), (φ_1,φ_2'), and so forth. The angles are randomly selected among $(0, \pi/8)$, $(0, 3\pi/8)$, $(\pi/4, \pi/8)$, and $(\pi/4, 3\pi/8)$, quickly enough to close the locality (*31*) and freedom-of-choice loopholes (Fig. 5A). We ran 1167 trials of the Bell test during an effective time of 1059 s. The data observed in the four settings are summarized in Fig. 5B, from which we found $S = 2.37 \pm 0.09$, with a violation of the CHSH-type Bell inequality $S \leq 2$ by four standard deviations. The result again confirms the nonlocal feature of entanglement and excludes the models of reality that rest on the notions of locality and realism—on a previously unattained scale of thousands of kilometers.

Concluding remarks

We have demonstrated the distribution of two entangled photons from a satellite to two ground stations that are physically separated by 1203 km and have observed the survival of entanglement and violation of Bell inequality. The distributed entangled photons are readily useful for entanglement-based quantum key distribution (*7*), which, so far, is the only way that has been demonstrated to establish secure keys between two distant locations with a separation of thousands of kilometers on Earth without relying on trustful relay. Another immediate application is to exploit the distributed entanglement to perform a variant of the quantum teleportation protocol (*32*) for remote preparation and control of quantum states, which can be a useful ingredient in distributed quantum networks. The satellite-based technology that we developed opens up a new avenue to both practical quantum communications and fundamental quantum optics experiments at distances previously inaccessible on the ground (*33*, *34*).

REFERENCES AND NOTES

1. A. Einstein, B. Podolsky, N. Rosen, *Phys. Rev.* **47**, 777–780 (1935).
2. E. Schrödinger, *Naturwissenschaften* **23**, 807–812 (1935).
3. C. S. Wu, I. Shaknov, *Phys. Rev.* **77**, 136 (1950).
4. S. J. Freedman, J. F. Clauser, *Phys. Rev. Lett.* **28**, 938–941 (1972).
5. A. Aspect, P. Grangier, G. Roger, *Phys. Rev. Lett.* **49**, 91–94 (1982).
6. J. S. Bell, *Physics* **1**, 195 (1964).
7. A. K. Ekert, *Phys. Rev. Lett.* **67**, 661–663 (1991).
8. C. H. Bennett *et al.*, *Phys. Rev. Lett.* **70**, 1895–1899 (1993).
9. H. J. Kimble, *Nature* **453**, 1023–1030 (2008).
10. J. Yin *et al.*, *Nature* **488**, 185–188 (2012).
11. W. K. Wootters, W. H. Zurek, *Nature* **299**, 802–803 (1982).
12. H.-J. Briegel, W. Dür, J. I. Cirac, P. Zoller, *Phys. Rev. Lett.* **81**, 5932–5935 (1998).
13. M. Zukowski, A. Zeilinger, M. A. Horne, A. K. Ekert, *Phys. Rev. Lett.* **71**, 4287–4290 (1993).
14. J.-W. Pan, C. Simon, C. Brukner, A. Zeilinger, *Nature* **410**, 1067–1070 (2001).
15. L. M. Duan, M. D. Lukin, J. I. Cirac, P. Zoller, *Nature* **414**, 413–418 (2001).
16. J.-W. Pan, D. Bouwmeester, H. Weinfurter, A. Zeilinger, *Phys. Rev. Lett.* **80**, 3891–3894 (1998).
17. J.-W. Pan, S. Gasparoni, R. Ursin, G. Weihs, A. Zeilinger, *Nature* **423**, 417–422 (2003).
18. C. H. van der Wal *et al.*, *Science* **301**, 196–200 (2003).
19. Z.-S. Yuan *et al.*, *Nature* **454**, 1098–1101 (2008).
20. C.-W. Chou *et al.*, *Science* **316**, 1316–1320 (2007).
21. S.-J. Yang, X.-J. Wang, X.-H. Bao, J.-W. Pan, *Nat. Photonics* **10**, 381 (2016).
22. M. Aspelmeyer *et al.*, *Science* **301**, 621–623 (2003).
23. C.-Z. Peng *et al.*, *Phys. Rev. Lett.* **94**, 150501 (2005).
24. J.-Y. Wang *et al.*, *Nat. Photonics* **7**, 387–393 (2013).
25. S. Nauerth *et al.*, *Nat. Photonics* **7**, 382–386 (2013).
26. The supplementary materials provide more details about payloads in the satellite, receiving ground stations, and the polarization compensation method, as well as relevant supporting data.
27. H.-L. Yin *et al.*, *Phys. Rev. Lett.* **117**, 190501 (2016).
28. K. Tsujikawa, K. Tajima, J. Zhou, *Opt. Fiber Technol.* **11**, 319–331 (2005).
29. B. B. Blinov, D. L. Moehring, L. Duan, C. Monroe, *Nature* **428**, 153–157 (2004).
30. J. F. Clauser, M. A. Horne, A. Shimony, R. A. Holt, *Phys. Rev. Lett.* **23**, 880–884 (1969).
31. G. Weihs, T. Jennewein, C. Simon, H. Weinfurter, A. Zeilinger, *Phys. Rev. Lett.* **81**, 5039–5043 (1998).
32. D. Boschi, S. Branca, F. De Martini, L. Hardy, S. Popescu, *Phys. Rev. Lett.* **80**, 1121–1125 (1998).
33. D. P. Rideout *et al.*, *Class. Quantum Gravity* **29**, 224011 (2012).
34. S. K. Joshi *et al.*, Space QUEST mission proposal: Experimentally testing decoherence due to gravity. arXiv:1703.08036 [math.FA] (26 April 2017).

ACKNOWLEDGMENTS

We thank many colleagues at the National Space Science Center, National Astronomical Observatories, and China Xi'an Satellite Control Center, especially B.-M. Xu, J. Li, J.-C. Gong, B. Chen,

J. Liu, X.-J. Jiang, and T. Xi for their management and coordination. We thank Q. Zhang, L. Li, and S. Chen for helpful discussions. This work was supported by the Strategic Priority Research Program on Space Science of the Chinese Academy of Sciences and by the National Natural Science Foundation of China. C.-Z.P. and J.-W.P. conceived the research. C.-Z.P., J.-Y.W., and J.-W.P. designed the experiments. J.Y., Y.C., G.-B.L., Z.-Q.J., M.L., C.-Z.P., and J.-W.P. developed the spaceborne entangled-photon source. J.Y., Y.C., S.-K.L., L.Z., W.-Q.C., G.-B.L., Z.-Q.J., M.L., J.-J.J., Y.-L.Z., Z.-C.Z., R.S., C.-Z.P., J.-Y.W., and J.-W.P. designed and developed the satellite and payloads. L.Z., J.-J.J., R.S., C.-Z.P., and J.-Y.W. developed the transmitters and the ATP technique. S.-K.L., W.-Q.C., W.-Y.L., and C.-Z.P. developed the software. J.Y., Y.C., L.Z., Y.-H.L., C.-Z.P., and J.-W.P. developed the polarization compensation method. C.-Y.L., C.-Z.P., and J.-W.P. analyzed the data and wrote the manuscript, with input from J.Y., Y.C., and Y.-H.L. All authors contributed to the data collection, discussed the results, and reviewed the manuscript. J.-W.P. supervised the whole project.

SUPPLEMENTARY MATERIALS

www.sciencemag.org/content/356/6343/1140/suppl/DC1
Materials and Methods
Figs. S1 to S11
Table S1
Reference (*35*)

28 March 2017; accepted 22 May 2017
10.1126/science.aan3211